2025-01-06

Stability of LiF Mirror Coatings on Space Telescopes at L2 Orbit

Devin M. Lewis
Brigham Young University

Stability of LiF Mirror Coatings on Space Telescopes at L2 Orbit

Devin M. Lewis

A thesis submitted to the faculty of
Brigham Young University
in partial fulfillment of the requirements for the degree of

Master of Science

David Allred, Chair
Richard Vanfleet
Richard Sandberg

Department of Physics and Astronomy

Brigham Young University

ABSTRACT

Stability of LiF Mirror Coatings on Space Telescopes at L2 Orbit

Devin M. Lewis
Department of Physics and Astronomy, BYU
Master of Science

A team at Goddard Space Flight center has developed a coating of aluminum mirrors they term XeLiF. This coating has high ultraviolet reflection and improved environmental stability over similar LiF coatings. For these reasons, it is a potential candidate for the future Habitable Worlds Observatory (HWO) flagship space telescope mission. However, the stability of XeLiF at the planned L2 orbit of HWO has not been investigated. This study highlights the potential damage to XeLiF when irradiated by electrons that will be present at L2. This radiation will begin removing LiF after 6 years of exposure as well as start roughening the surface. An RMS roughness over 40 nm will be reached by 30 years. Protective measures or replacement coatings need to be investigated.

Keywords: LiF, HWO, radiation damage, L2 orbit, SEM

ACKNOWLEDGMENTS

First and foremost I would like to thank Dr. Allred for his continued support and council while doing this research. He pushed me to find the answers to questions that interested me while studying these materials.

The input and guidance from Dr. Vanfleet on this project was vital. I greatly appreciate all his time and effort in helping me with this project and look forward to co-authoring on a future paper from this work.

Thank you to Paul Minson and everyone in the Electron Microscopy facility for their advice, assistance, and access to equipment.

Everyone on the coatings team at Goddard Space Flight Center that I was privileged to work with: Manuel Quijada, Luis Rodriguez de Marcos, Javier del Hoyo, and Mateo Batkis. Thank you for providing the samples that made this whole experiment possible as well as the feedback through the whole process.

Much appreciation to the funding sources that supported me and my education during this research, as well as made it possible to present at multiple conferences.

Funding from Brigham Young University and NASA UNSGC 80NSSC20M0103.

Contents

Chapter 1

Introduction

The habitable worlds observatory (HWO) is a concept flagship space telescope mission with the dedicated purpose of searching for exoplanets that potentially contain life [1]. To do so, this telescope will be capable of observations over the far ultraviolet (FUV) to infrared range. The optimal reflector for this range is an aluminum (Al) mirror, which is an excellent broadband reflector and higher FUV reflectance than other common reflectors (Au or Ag) [2]. Al_2O_3 readily grows on Al surfaces when exposed to oxygen. Even a few nm of Al_2O_3 will absorb wavelengths shorter than 140 nm [3]. To prevent the growth of Al_2O_3, and the subsequent absorption of light, a metal fluoride capping layer will be deposited on top of the Al.

LiF has the highest UV transparency [4] and is thus a desirable coating as far as optical performance goes. However, LiF's hygroscopic nature makes it challenging to work with since the fabricated mirrors spend years at a moderate exposure to humidity. Clean rooms are kept around 45% relative humidity (RH) to prevent charging and damage of electronic components, as well as most launch sites are in locations with high average humidities.

Goddard Space Flight Center (GSFC) has developed a new coating procedure of LiF that they report to have a much higher resistance to humidity. Their process involves an initial fluorination of the Al mirror by passivating with XeF_2 gas. This creates a thin (2-3 nm) AlF_3 film on the surface.

LiF is then deposited by conventional thermal evaporation followed by another XeF_2 passivation cycle. This final cycle is done to heal any defects and reduce the amount of pinholes. Traditionaly deposited LiF is done onto a heated substrate, but the healing effect of the final passivation step removes this requirement, which reduces one level of complexity of the deposition process. GSFC has termed this new formulation Al+XeLiF. Environmental testing demonstrated that this coating is much more resilient than traditionally deposited LiF and will exhibit minimal change when stored in a cool environment (3 °C) [5, 6].

Now that a mirror coating has been found with higher stability in its storage environment on earth, its stability in space needs to be investigated. HWO is planned to operate at the L2 orbit, a location where surfaces will be bombarded by energetic particles across a large spectrum of energies. While it is crucial to understand the effect of both the ions and electrons these coatings will be bombarded with, for the scope of this project I focused on the effect electrons will have on the HWO mirrors at L2.

1.1 Previous Work

I assisted GSFC in a previous environmental study of Al+XeLiF by characterizing film changes when exposed to different temperatures and humidities over a period of six months [6]. In this study, I attempted to use a scanning electron microscope (SEM) as one method of characterization. However, while attempting to image the sample I watched the surface degrade and appear to bubble up. I recorded this sequence and it is displayed in Fig. 1.1. In this case the microscope was being operated with a beam energy of 3 keV and a beam current of 50 pA. While the electron energies and flux in the SEM are different from those in space, it may be representative of the degradation that may occur.

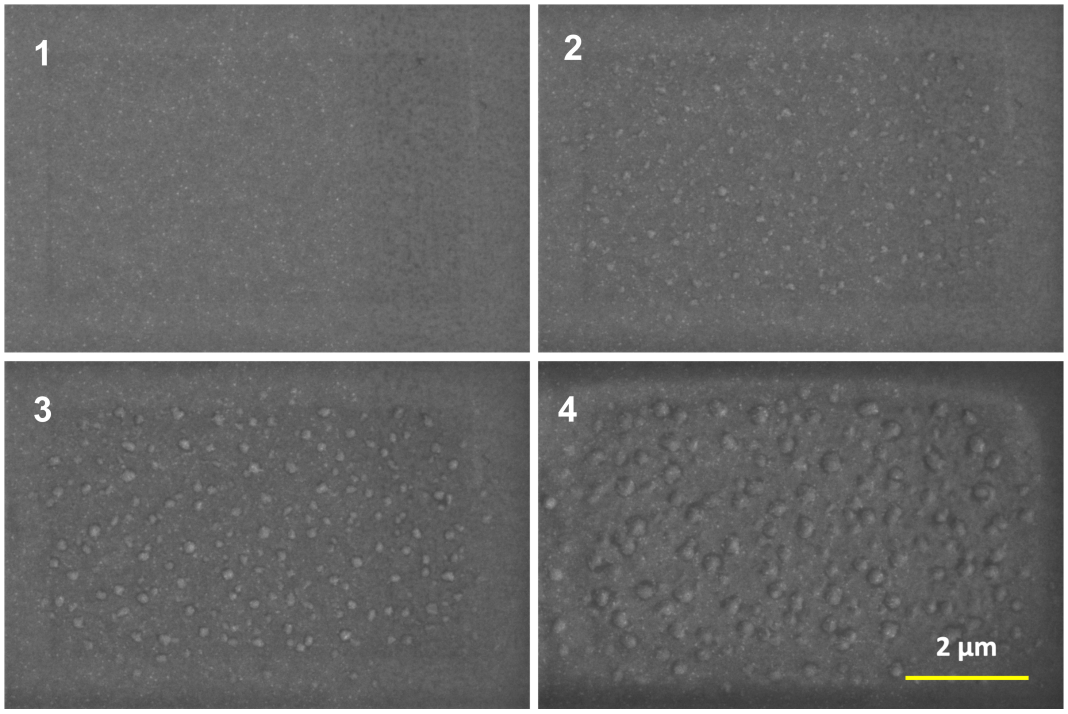

Figure 1.1 Sequence of SEM images of Al+XeLiF sample showing film sensitivity to the electron beam. Between each image the sample was irradiated with the electron beam (3 keV, 50 pA) for approximately 1.5 minutes.

While this visible level of deterioration may not be significant to overall reflection (it has yet to be tested), the resulting roughening of the surface may be catastrophic if Al+XeLiF were used on HWO. From an arbitrarily assigned error budget it was derived that there would be a limit of 1 nm rms roughness on the primary mirror [7]. More recently H. Philip Stahl *et al.* [8] discussed that the limiting factor for the acceptable near-angle scatter of the coronograph is a combination of the correlation length with the rms roughness on the primary mirror. As the exact error budget and roughness limitations become more precisely determined, it will be essential to understand the potential roughening that will occur in orbit. Many of the larger features seen in Fig. 1.1-4 are approximately 200 nm in diameter. Depending on their height, they may be the cause of scattering significant enough to disqualify LiF for use on HWO.

1.2 Environment at L2 Orbit

Charged particles in space come from several origins, mainly the solar wind, coronal mass ejections (CME), and galactic cosmic rays (GCR). Depending on the orientation of the telescope and levels of shielding, different sources will be more prevalent. Minow *et al.* [9] used a model they developed entitled the L2 charged particle environment (L2-CPE) model, to estimate the fluence of charged particles in the sunward and anti-sunward directions at the L2 orbit. Fluence is the total flux per unit area integrated over a period of time. In the case of electron bombardment on a surface in space, the fluence would be the number of electrons per unit area over a set period of time. Fig. 1.2 shows the modeled max electron fluence (electrons/m^2 at L2 Minow *et al.* reported, over a year period for both sunward and anti-sunward facing surfaces.

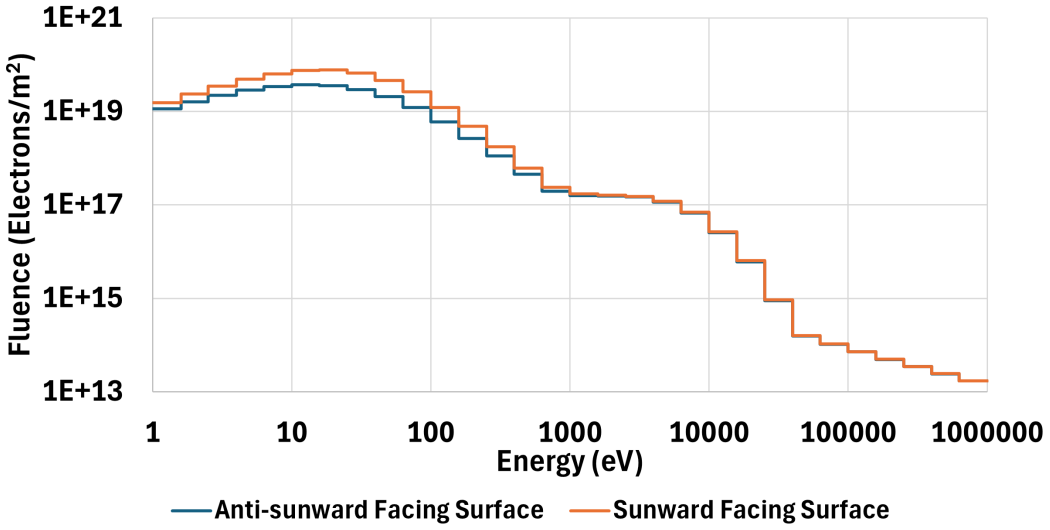

Figure 1.2 Log-log graph of the max one year electron fluence (integrated flux) at the L2 orbit for sunward and anti-sunward facing surfaces.

As might be expected, Fig. 1.2 shows that surfaces facing the sun experience higher fluence of electrons. However, anti-sunward facing surfaces have the same order of magnitude of fluence as sunward facing surfaces, so they can be treated as roughly the same since the data is viewed on a

log-log scale. This means simply pointing the telescope away from the sun may be insufficient in protecting mirror surfaces.

Also of note is the distribution of electrons across the energy spectrum. There are several orders of magnitude more low energy electrons than high energy. Understanding if the electron energy has an affect on film degradation will be crucial in this experiment.

1.3 Effect of Low Energy Electrons

High energy particles (on the order of 1 MeV) are often of more concern as they can penetrate deep into materials where they deposit the majority of their energy. This is the case when considering shielding requirements for electronics or protecting astronauts on a mission. However, low energy particles (100's of eV) are more concerning for mirrors and thin films because they will deposit their energy within the thin mirror coatings. Fig. 1.3 shows Monte Carlo simulations of electron interactions in an Al+XeLiF sample. The simulations were done using Casino V2.4.8.1 software with the film thicknesses of this study. The AlF_3 and LiF film thicknesses match what would be done on HWO. Fig. 1.3 demonstrates that electrons at 700 eV and lower will have their entire interaction volume contained within the LiF layer. It also shows that electrons with higher energy (5 keV or more) will interact and deposit the majority of their energy in underlying layers with fewer interactions in the LiF. This is cause for concern since the majority of electron fluence seen in Fig. 1.2 is <1 keV.

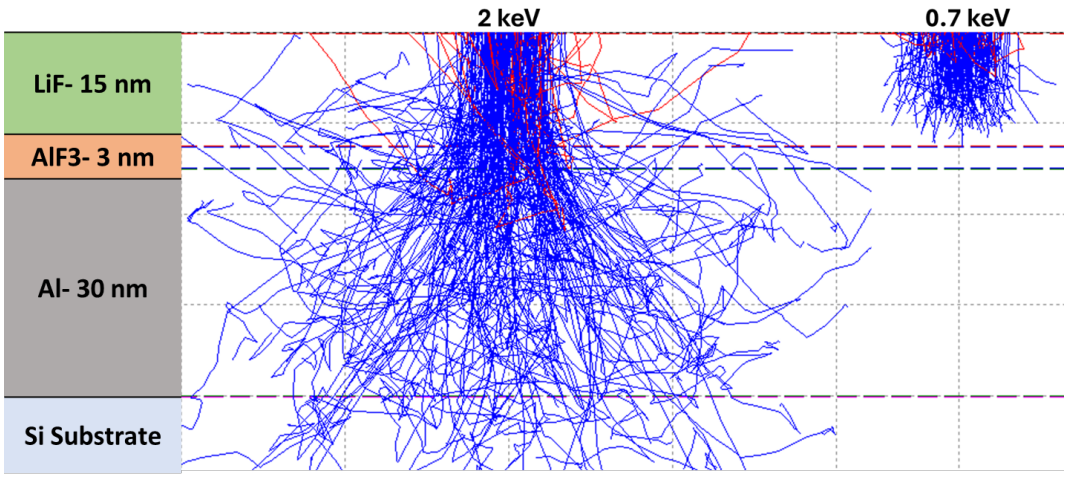

Figure 1.3 Monte Carlo simulation of electron interactions in Al+XeLiF sample. Two energies were simulated. Electrons with a landing energy of 2 keV (left) and 700 eV (right). The red lines are backscattered electrons that escape the sample. The film stack matches the GSFC samples used in this study.

Chapter 2

Experimental

An 8-inch Si (100) wafer was sent to GSFC to be used as a substrate in their Al+XeLiF deposition process. This maximized the number of samples that could be cleaved from the initial wafer to run multiple experiments. GSFC followed the same deposition procedure as described above and further information and parameters can be found in Quijada *et al.* [10, 11] reports. The target thicknesses were 30 nm Al, 3 nm AlF_3, and 15 nm LiF. The Al is notably thinner than what would eventually be flown. This was done for a separate optical study but as the LiF layer is the primary interest of this study, the Al being optically thin should have no affect on the results of this study.

The sample was shipped in a nitrogen purged box to minimize any damage from humidity in transit. The wafer was cleaved into approximately 1x1 inch pieces and stored in a desiccator (<12% relative humidity at 21°C) between measurements. GSFC's evaporation chamber is configured for a 4x4 inch deposition region, so some thickness non-uniformity is expected across the surface of the wafer. This will affect some direct numerical comparisons between samples, and so care was taken when choosing samples to perform these experiments on regions that were close in proximity.

2.1 SEM

An SEM was used to both degrade samples and quantify the damage. The SEM allows for precise irradiation and energy selection as well as elemental analysis through energy dispersive x-ray analysis (EDX). However, before the experiment could commence, beam settings had to be determined. Eq. 2.1 was used to calculate the electron fluence samples undergo in the SEM.

$$(6.24 \times 10^{18})\frac{It}{A} electrons/m^2 \tag{2.1}$$

Where I is the beam current in amps, A is the area of the irradiated region in m^2, and t is the exposure time in seconds. The number of electrons per coulomb (6.24×10^{18}) is used to convert amps to electrons per second. This allowed exact fluences to be selected for study.

Precise electron fluence data at L2 was not available at the beginning of this experiment, only a less detailed version of the data seen in Fig. 1.2. So, fluences that appeared to be above max values in the early version of Fig. 1.2 were selected. A starting fluence of 6.85×10^{19} electrons/m^2 was chosen and also used as the step size when increasing total fluence in an exposure.

Now that more exact fluence estimates are available, it is seen that sunward and anti-sunward facing surfaces have max fluences of 7.7×10^{19} and 3.6×10^{19} electrons/m^2 respectively at about 20 eV, as seen in Fig. 1.2. This means that for surfaces facing away from the sun, it would take more than a year of irradiation to reach a fluence of 6.85×10^{19} electrons/m^2, regardless of the energy. However, this information will still be useful, as it will provide an estimate to what will happen to the film over its many year life span at L2.

To control the fluence in the SEM, the beam current and area of exposure were kept constant while varying time. This allowed the fluence to be altered at different selected beam energies of interest. The 6.85×10^{19} electrons/m^2 was achieved by irradiating a region 8.3 μm wide and 5.5 μm tall (45.6 μm^2) for 10 s with a beam current of 50 pA. The exposure time was increased in 10 s increments for up to 16 different regions at a single energy. Increasing the exposure time

in 10 s increments increased the fluence in increments of 6.85×10^{19} electrons/m^2. Fig. 2.1 is an SEM image of a patterned region after irradiation exposures but before EDX spectra were taken. The beam was also blanked between exposures and while driving the stage to avoid any incidental exposure.

After sample irradiation a sequence of EDX spectra were taken. Fig. 2.1 the regions inside the previously irradiated areas where EDX would be taken. The process of collecting EDX spectra will also damage the sample. To keep the amount of damage consistent between scans all EDX spectra were always taken with a beam accelerating voltage of 5 kV and a beam current of 50 pA. Additional care was taken to make the scan regions as close in size as possible, however some variability in scan size was inevitable.

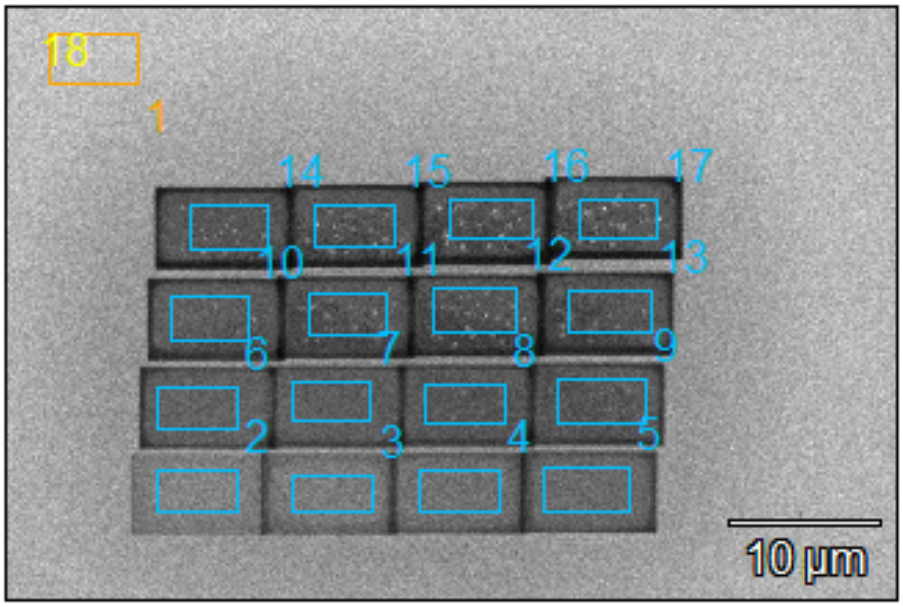

Figure 2.1 SEM image of sample after irradiation but before EDX spectra were taken. This sample was irradiated with fluences from 6.85×10^{19} to 1.10×10^{21} electrons/m^2 at 5 keV. The higher numbers correspond with regions exposed to progressively longer irradiation times (10 s increments) with 1 being a control.

The SEM used to irradiate and study the XeLiF samples was a ThermoScientific Verios G4 UC SEM equipped with an UltraDry Premium EDS detector.

2.2 AFM

Low surface roughness is crucial for the successful operation of the coronograph on HWO and so understanding the observed sample coarsening via is by extension, also necessary. Atomic force microscopy (AFM) was an available technique that allows direct measurement of the surface roughness of the sample. To understand the effects of the observed coarsening, samples were first irradiated in the SEM and then measured on the AFM.

The available AFM used a small optical microscope to assist in stage stearing and finding regions of interest on the sample surface. This made locating irradiated regions difficult, as they had to be large enough to see in this scope. For this portion of the experiment, the irradiated areas were approximately 3.3 mm^2 since anything smaller was difficult to find on the AFM. This in turn made it take much longer (30 min) to get to the same fluences observed in EDX because of the area dependence seen in Eq. 2.1. Because of limited time and resources, only two electron energies were studied(50 and 100 eV).

The AFM used for this experiment was a Veeco™ Dimension 5000, with Aspire™ conical AFM tips, part number CT300R-25. Gwyddion open source software was then used to analyze the collected data.

2.3 XPS

X-ray photoelectron spectroscopy (XPS) was an additional technique to study the mechanism of damage. It is possible that the damage seen in Fig. 1.1 is the result of chemical change. XPS is capable of detecting such chemical shifts and should help in understanding the mechanism of degradation. A large area, as done for AFM(3.3 mm^2 to 6.3×10^{20} electrons/m^2), was irradiated in the SEM. XPS measurements were made of the irradiated and non-irradiated regions. Broad scans

were taken of the whole available scan and focused scans of the expected elements were taken for more precise comparisons.

The XPS used in this experiment was a Thermo Fisher Scientific SSX-100 with an Al kα source and a hemispherical analyzer. CasaXPS software was used to analyze the collected data.

2.4 TEM

In an attempt to better understand the mechanism of LiF destruction transmission electron microscopy (TEM) was done on a cross-section of an irradiated region. The sample was first irradiated to a fluence of 6.2×10^{20} electrons/m^2 at a beam energy of 500 eV. The sample was then coated with additional layers of gold and platinum to protect from the milling process. A lamella was then milled out using focused ion beam (FIB) milling and then imaged with an FEI Tecnai F20 TEM.

Chapter 3

Results and Discussion

3.1 EDX Results

At the selected beam energy for collecting EDX spectra (5 keV), the beam interaction volume extended into all layers of the film stack. This produces an EDX spectra with elemental signal from all present materials aside from Li, which EDX does not measure. Fig. 3.1 is one of the obtained EDX spectra, and it shows all expected elements. The C signal comes from surface contaminants and electron beam deposited C, commonly seen in electron microscopes. The AlF_3 contributes to both the F and Al signals, where the LiF, metal Al, and Si substrate contribute only to the F, Al, and Si signals respectively.

When taking EDX spectra at different fluence levels, the only signal seen to change was F counts. For this reason, F was tracked and plotted at all energies experimented on, seen in Fig. 3.2. This data provides information on a removal of LiF and a minimum energy requirement before change can occur.

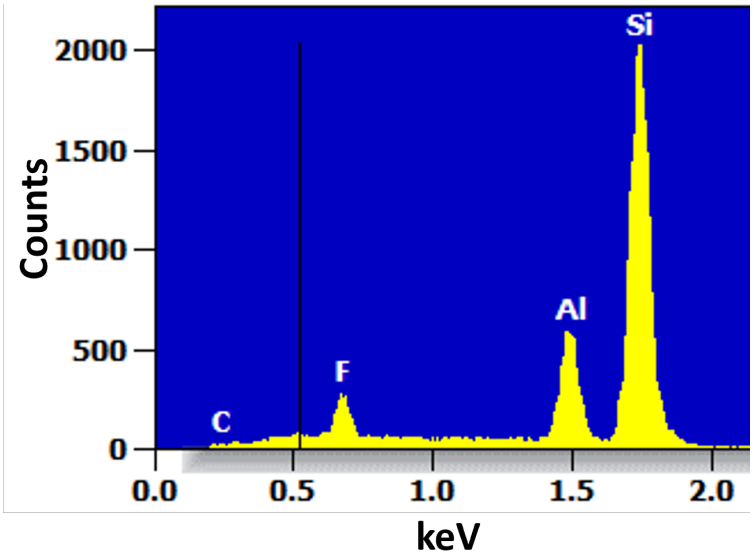

Figure 3.1 EDX spectra of Al+XeLiF sample region with no prior beam irradiation. The line at 0.525 keV is where an oxygen peak would be if present.

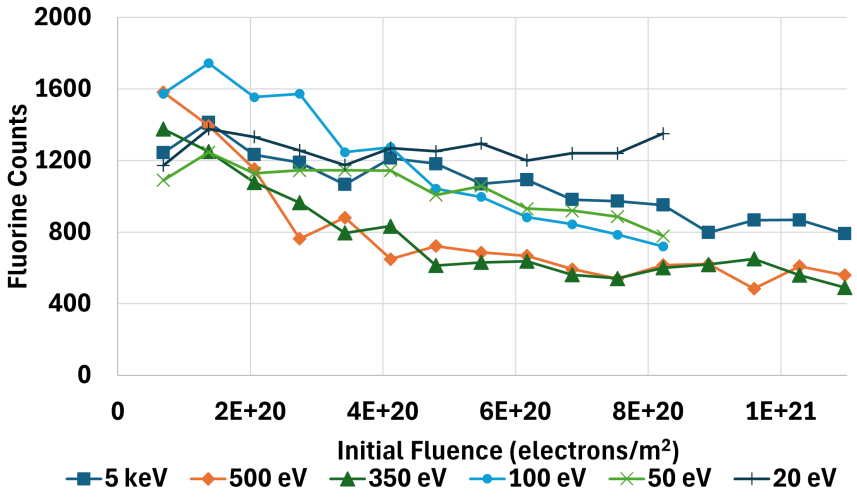

Figure 3.2 Fluorine counts from EDX spectra of Al+XeLiF sample after irradiation at different beam energies and fluences. The x-axis charts the amount of irradiation prior to EDX. The EDX was done at 5 keV and 50 pA with 100 s collection time.

3.1.1 Removal of LiF

There is no way to differentiate between F signal coming from LiF or AlF_3. In a previous experiment of metal fluoride stability under the electron beam of the SEM, I observed that AlF_3 was more stable than LiF. EDX in that case showed that pure LiF was removed but the electron beam did not appear to affect AlF_3. So, in the case of Al+XeLiF where AlF_3 and LiF are both present, a drop in F signal is interpreted as removal of the LiF.

The rate of LiF removal is seen to change at different beam energies. As predicted, lower energy electrons (<700 eV) do more damage to the LiF as seen in Fig. 3.3. The 5 keV electrons remove LiF slower than both the 350 and 500 eV electrons. Despite the difference in energy between 350 and 500 eV, they appear to remove LiF at the same rate.

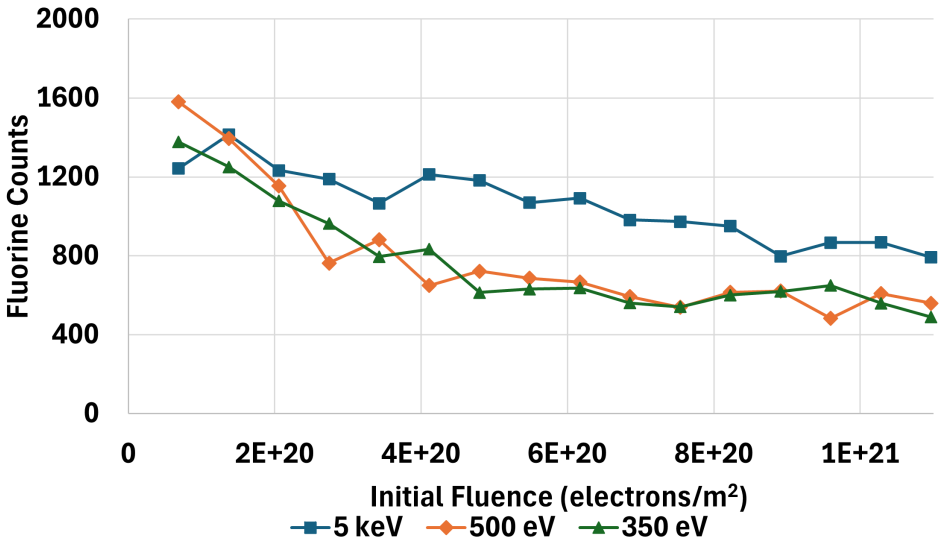

Figure 3.3 Selection of energies (5 keV, 500 eV, and 350 eV) from Fig. 3.2 for comparison. The shallower slope in the 5 keV run indicates that higher energy electrons damage LiF at a slower rate.

There also appears to be leveling out past 4×10^{20} electrons/m^2 for the cases 350 and 500 eV irradiation. This is likely occurs from one of two reasons. Either complete removal of the LiF

meaning all F signal now corresponds to the underlying AlF_3, or any remaining LiF has entered a stable state, resistant to damage from the electron beam.

3.1.2 Minimum Energy Requirement

At even lower energy radiation, the rate of LiF removal continues to drop. Fig. 3.4 is a selection of data from Fig. 3.2, displaying this. The lines corresponding to 50 and 100 eV irradiation have shallower slopes the 350 eV irradiation. The 350 eV data was kept in both Fig. 3.3 and Fig. 3.4 as a referentce between each other. As seen in Fig. 1.3 lower energy electrons have fewer interactions as well as less energy to be absorbed in general. This is likely the cause for the reduction in LiF removal rate as observed at 50 and 100 eV.

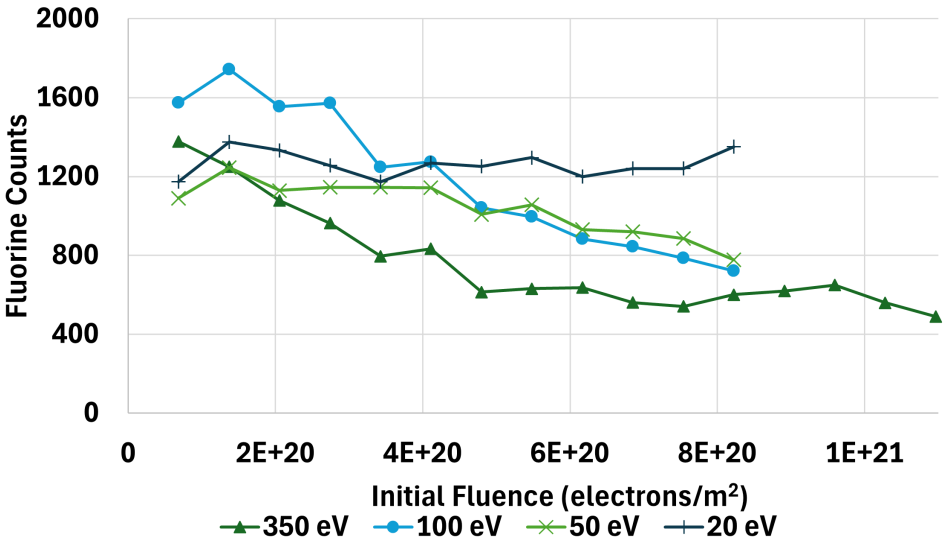

Figure 3.4 Selection of energies (20, 50, 100, and 350 eV) from Fig. 3.2 for comparison. Fluorine counts from EDX spectra taken from different fluence exposures. The flat 20 eV line indicates that no LiF was removed from this region. The shallower slopes on the 50 and 100 eV lines show that LiF is being removed at a slower rate than the 350 eV exposure.

It is also seen that there is an energy where no LiF was removed (20 eV). This supports the idea that there is some activation energy required before damage can occur. Operating the SEM at beam

energies lower than 100 eV is challenging as well as there is uncertainty in the exact beam energy because the beam is not perfectly monochromatic. From this data I estimate the exact threshold energy is somewhere between 20-50 eV.

3.2 AFM Results

It was difficult to find damaged regions on the AFM unless they were fully deteriorated and the irradiated region was large. This limited the number of different fluences that could easily be studied on the AFM. For this reason only 50 and 100 eV beam energies were studied. Two regions were irradiated to a fluence of 6.3×10^{20} electrons/m^2 with the selected beam energies. An optical photograph of the sample after this irradiation is shown in Fig. 3.5. Other irradiated areas are seen in the figure as well. These are where beam alignments or other tests took place, but it was difficult to find any areas of interest smaller than regions A or B on the AFM.

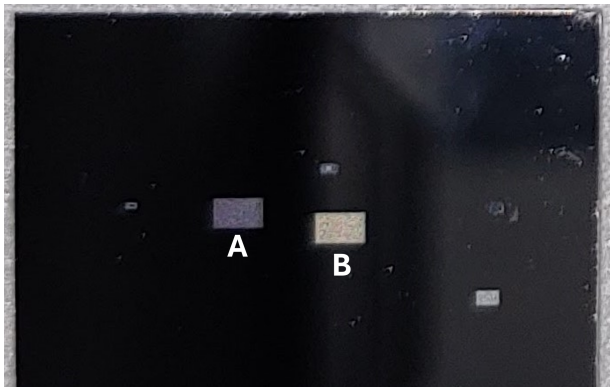

Figure 3.5 Optical photograph of XeLiF sample that was used for AFM scans. Regions A and B are where the sample was irradiated at 50 and 100 eV respectively. These regions were irradiated to 6.3×10^{20} electrons/m^2 and are approximately 2.5 mm wide. Other irradiated areas are seen where beam allignments or other tests took place, but it was difficult to find any regions smaller than A or B on the AFM.

AFM scans of these regions are shown in Fig. 3.6. Both scans have an RMS roughness over 40 nm which far exceeds the error budget of 1 nm RMS. While this is concerning, of separate note

is the sheer size of defects on the surface. In both scans features appear to be approximately 1 μm in diameter and over 300 nm in height. This raises the question of how this mirror's reflection is affected. The irradiated regions as seen in the optical image in Fig. 3.5 are brighter than the rest of the mirror, suggesting high optical scattering. This means that mirror is compromised in at least the optical spectrum, and likely the FUV range as well. For exact quantification, detailed reflection data needs be collected.

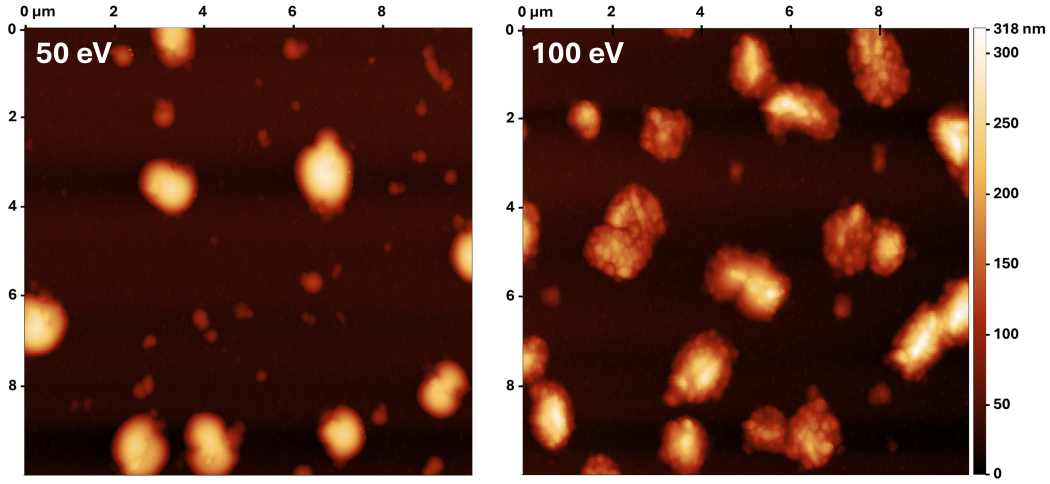

Figure 3.6 AFM scans of 10x10 μm regions irradiated with a fluence of 6.3×10^{20} electrons/m^2 at 50 eV (left) and 100 eV (right). The 50 eV region had an RMS roughness of 44 nm and the 100 eV region was 54 nm RMS. The size and height of features are approximately the same, but the frequency of occurrence appears much higher in the 100 eV exposure.

3.3 XPS Results

Wide XPS spectra showed no unexpected elements in either the irradiated or non-irradiated regions, just Li, C, O, F, Al, and Si. Fig. 3.7 are focused scans of Li and F of both irradiated or non-irradiated regions. Most apparent is the drop in signal in the irradiated region. This supports that there is a general removal LiF. According to Fig. 3.3, a fluence of 6.3×10^{20} electrons/m^2 at 350 eV would

put the sample in stable state. Together, this supports that the remaining LiF has entered a stable state where the LiF is no longer removed.

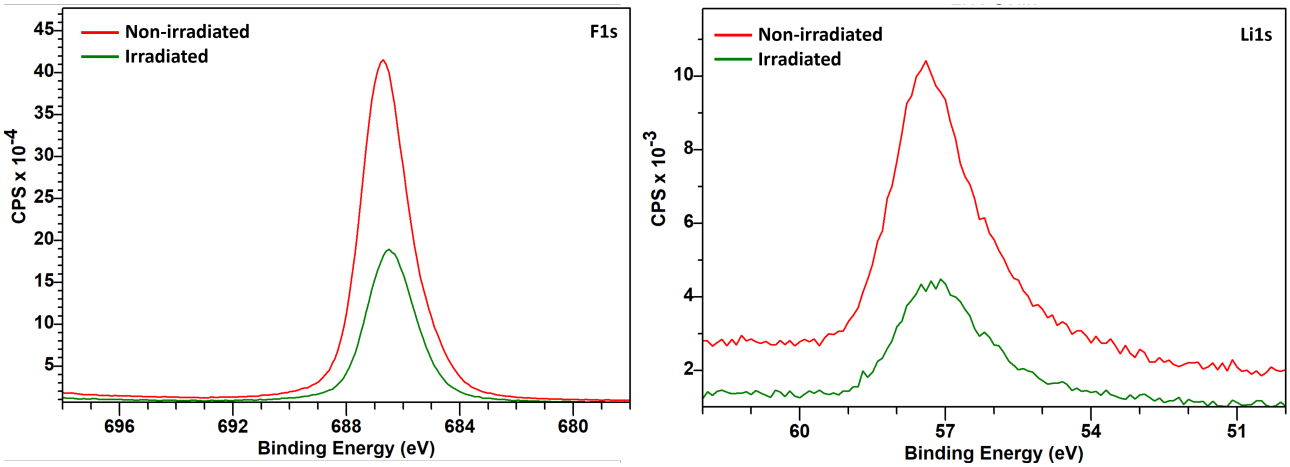

Figure 3.7 XPS spectra of F1s (left) and Li1s (right) scans of irradiated and non-irradiated regions. The irradiated region was exposed to a fluence of approximately 6.3×10^{20} electrons/m^2 at 350 eV.

Secondly, there is no shift in position in either Li or F. This means that LiF does not change into another chemical form. One original hypothesis for the mechanism of degradation was that LiF was broken down, leaving Li metal as F is pumped off in a gaseous form. But, Fig. 3.7 shows that this is not the case and that LiF molecules are removed entirely, leaving no Li or F behind.

3.4 TEM Results

XPS showed that stable LiF remains on the sample and ideally, TEM would determine where the LiF is located. However, this was not the case.

A TEM cross section of one raised features is seen in Fig. 3.6. This sample had been previously irradiate to 6.2×10^{20} electrons/m^2 at 500 eV. The highlighted red region is where an EDX spectra was taken, which is shown in Fig. 3.9.

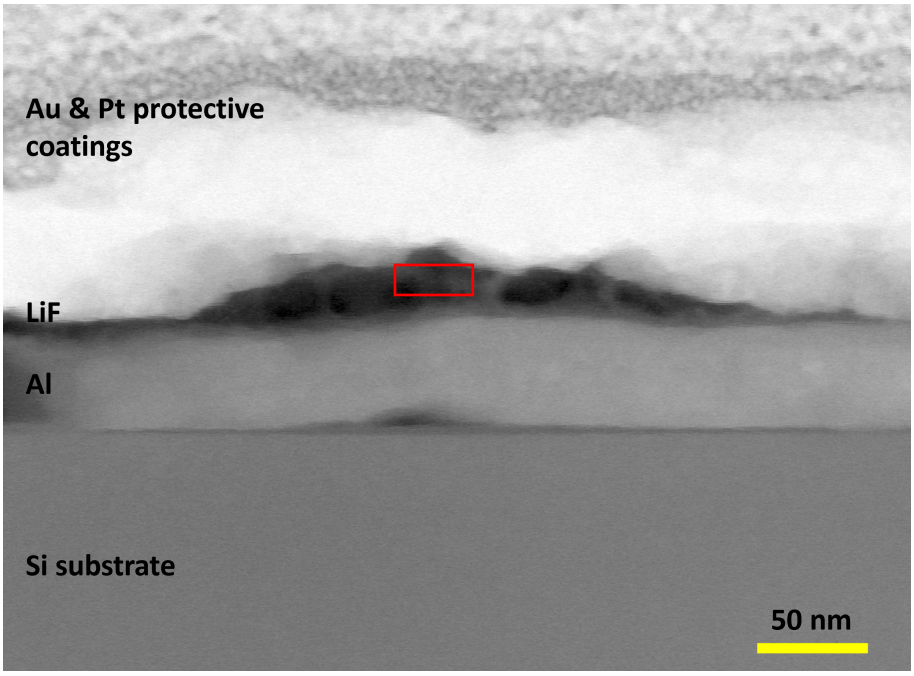

Figure 3.8 TEM micrograph of a cross-section of one of the raised bumps seen in AFM. There appears to be a thinning of the LiF on the sides of this feature. This region had been irradiated with a fluence of 6.2×10^{20} electrons/m^2 at 500 eV. The labels identify the corresponding layers in the film stack.

The EDX spectra has low total counts, only one tenth of total counts when compared to surrounding regions. This is likely from large amounts of voids in this region, suggesting that the top film and domed feature were unstable during the FIB milling process. The EDX spectra also has higher C counts compared to other regions. This could be from the SEM exposure, which deposits C on scanned surfaces, but it also might be a part of the damage process.

Unfortunately no significant F was measured in any regions of the TEM micrograph. This further supports that the remaining LiF was not stable during FIB processing, even though XPS showed that LiF reached a stable state in the SEM. This made locating the remaining LiF via TEM impossible in this case.

While the EDX data did not provide the desired information on the stable LiF, two main observations could still be made from the TEM micrograph in Fig. 3.8. First is a thinning of

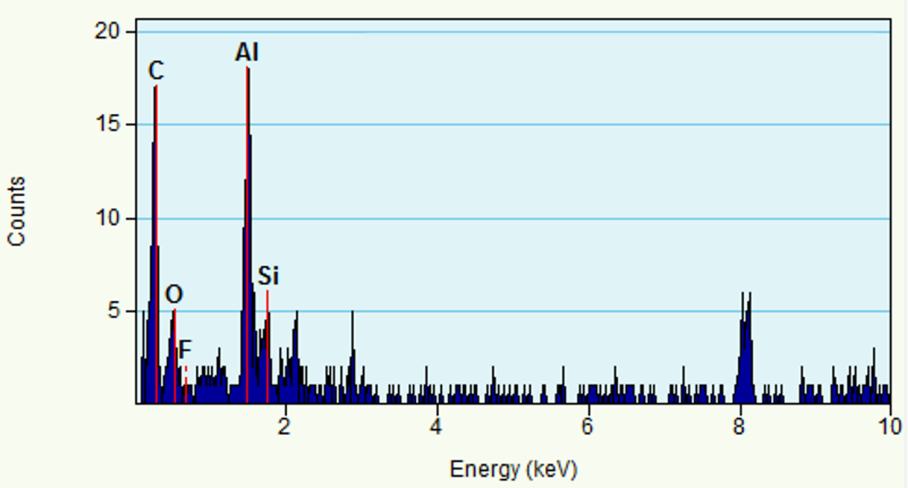

Figure 3.9 EDX spectra of the red highlighted region in Fig. 3.8. There are low total counts suggesting mostly void in this region. Carbon is slightly higher than other regions.

apparent LiF around a raised dark feature. This could be from a combination of LiF removal as well as a reorganization of the LiF into a more stable mass. EDX was done on the region to potentially identify the materials, but unfortunately, the FIB milling process appeared to remove all the material near the surface, leaving an outline behind.

The second observed feature was the dark bump below the Al layer. A feature like this was seen under every raised bump that was observed. It could possibly be Al delamination, further weakening the film, but its exact nature is unknown. For a better understanding more TEM measurements should be taken in the future.

Chapter 4

Conclusions

4.1 Lifetime of XeLiF

In order to calculate the time needed to reach the shown degradation levels, the electrons in the affecting energy range from the L2-CPE needs to be summed. To understand that range, Fig. 4.1 was drawn up as a possible representation from the information derived from Fig. 3.3 and Fig. 3.4. Picking the limits to sum across is difficult because of the changing rates of damage, so the choice is somewhat arbitrary. In this case it was decided to sum the electrons from 50-5000 eV, for 2.33×10^{19} electrons/m^2 after one year of exposure. The L2-CPE data for anti-sunward facing was used, as HWO likely will never face the sun.

Dividing the fluence exposure that was done in the SEM by the summed fluence amount then gives the length of time, in years, in space required to reach that level of degradation. The large roughening seen in the AFM scans in Fig. 3.6 would happen in 27 years. Putting this time scale on the EDX results in Fig. 3.2 gives a 3-year step between each data point. Again, because collecting the EDX spectra continues to damage the sample it is hard to get a lifetime before complete LiF

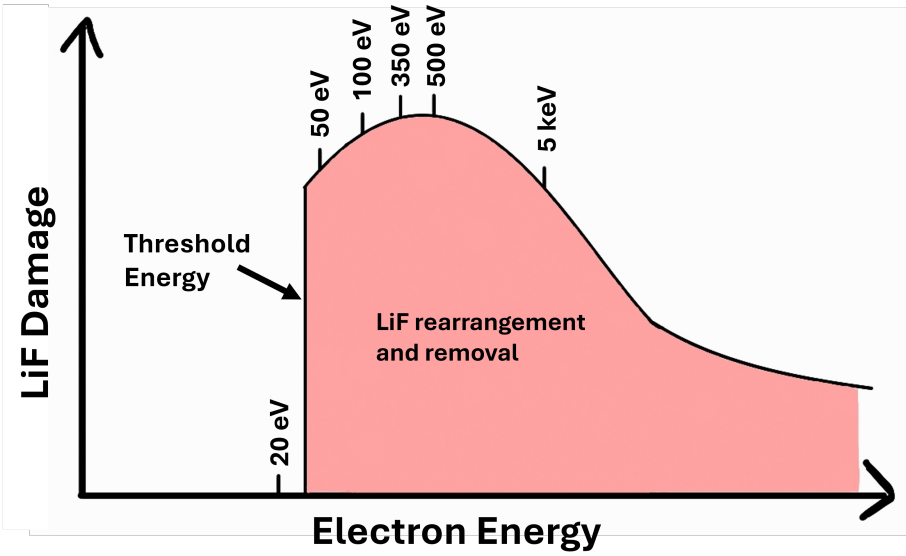

Figure 4.1 A possible model drawn to demonstrate the changes in rates of degradation between electron energy levels. There is also some threshold energy level required before any damage is observed.

removal. The first data point in Fig. 3.2 is after an initial equivalent 3-year exposure. So, after 6 years of exposure, at least some LiF will be removed.

This puts a big limitation on Al+XeLiF being used for HWO, before any kind of ion radiation testing has been done. This is a cause for some concern, especially if the mission lasts many years. In comparison, Hubble has been operating for 30 years, a length of time HWO likely would not achieve with this coating.

4.2 Possible Solution

There a few possible solutions that warrant further investigation looking forward. The LiF could be coated with a different metal fluoride that is resilient to charged particle radiation. It that would absorb the more numerous low energy electrons and protect the underlying LiF. Initial observations of MgF_2 and AlF_3 under the SEM show them to be significantly more stable than LiF. If protecting

the LiF proves too challenging, LiF may have to be entirely replaced by MgF_2, AlF_3, or some other material entirely. No matter the path going forward, the current formulation of Al+XeLiF coating alone, will likely be insufficient.

Bibliography

[1] *Pathways to Discovery in Astronomy and Astrophysics for the 2020s* (National Academies Press, 2023).

[2] D. Y. Smith, E. Shiles, M. Inokuti, and E. D. Palik, "The Optical Properties of Metallic Aluminum," in *The Handbook of Optical Constants of Solids*, E. D. Palik, ed., (Academic Press, Orlando, FL 32887, Florida, USA, 1985), Vol. one, pp. 369–406.

[3] F. Gervais, "Aluminum Oxide (Al_2O_3)," in *Handbook of Optical Constants of Solids*, E. D. Palik, ed., (Academic Press, Boston, 1998), pp. 761–775.

[4] "Chapter 3 - Thermo-Optic Coefficients," in *Handbook of Optical Constants of Solids*, E. D. Palik, ed., (Academic Press, Burlington, 1997), pp. 115–261.

[5] M. A. Quijada, J. G. D. Hoyo, L. V. R. de Marcos, E. J. Wollack, M. F. Batkis, D. M. Lewis, T. D. Rydalch, and D. D. Allred, "Enhanced far ultra-violet optical properties of physical vapor deposited aluminum mirrors through fluorination," In *Space Telescopes and Instrumentation 2024: Ultraviolet to Gamma Ray*, J.-W. A. den Herder, S. Nikzad, and K. Nakazawa, eds.,**13093,** 1309340 (SPIE, 2024).

[6] D. M. Lewis, T. D. Rydalch, D. D. Allred, L. R. de Marcos, M. A. Quijada, J. del Hoyo, and M. Batkis, "Stability of XeF2 passivated Al plus LiF as possible coating for HWO," In *Advances*

in Optical and Mechanical Technologies for Telescopes and Instrumentation VI, R. Navarro and R. Jedamzik, eds.,**13100,** 131000K (SPIE, 2024).

[7] H. P. Stahl, "Assessment of near-angle scatter on exo-Earth coronagraphy," In *UV/Optical/IR Space Telescopes and Instruments: Innovative Technologies and Concepts XI*, A. A. Barto, F. Keller, and H. P. Stahl, eds.,**12676,** 1267608 (SPIE, 2023).

[8] H. P. Stahl, D. D. Smith, and B. Nemati, "Impact of near-angle scatter on exo-Earth coronagraphy," In *Space Telescopes and Instrumentation 2024: Optical, Infrared, and Millimeter Wave*, L. E. Coyle, S. Matsuura, and M. D. Perrin, eds.,**13092,** 1309265 (SPIE, 2024).

[9] E. M. W. Joseph I. Minow, Anne M. Diekmann and V. N. Coffey, "L2-Charged Particle Environment (L2-CPE) Low Energy Radiation Fluence Model," In *Annual RADiation and its Effects on Components and Systems Conference 2023*, (2023).

[10] M. A. Quijada, J. del Hoyo, D. R. Boris, and S. G. Walton, "Improved mirror coatings for use in the Lyman Ultraviolet to enhance astronomical instrument capabilities," In *UV/Optical/IR Space Telescopes and Instruments: Innovative Technologies and Concepts VIII*, H. A. MacEwen and J. B. Breckinridge, eds.,**10398,** 103980Z (SPIE, 2017).

[11] M. A. Quijada, L. V. Rodriguez de Marcos, J. G. Del Hoyo, E. Gray, E. J. Wollack, and A. Brown, "Advanced Al mirrors protected with LiF overcoat to realize stable mirror coatings for astronomical telescopes," In *Advances in Optical and Mechanical Technologies for Telescopes and Instrumentation V*, R. Geyl and R. Navarro, eds., (SPIE, 2022).